Cancer Letters 410 (2017) 201–211

Contents lists available at ScienceDirect

Cancer Letters

journal homepage: www.elsevier.com/locate/canlet

Original Article

Targeting COPZ1 non-oncogene addiction counteracts the viability of thyroid tumor cells☆

Maria Chiara Anania [a], Elena Cetti [a], Daniele Lecis [a], Katia Todoerti [b], Alessandro Gulino [c], Giuseppe Mauro [a], Tiziana Di Marco [a], Loredana Cleris [a], Sonia Pagliardini [a], Giacomo Manenti [d], Beatrice Belmonte [c], Claudio Tripodo [c], Antonino Neri [e, f], Angela Greco [a, *]

[a] Department of Experimental Oncology and Molecular Medicine, Fondazione IRCCS Istituto Nazionale Dei Tumori, Milan, Italy
[b] Laboratory of Pre-Clinical and Translational Research, IRCCS-CROB, Referral Cancer Center of Basilicata, Rionero in Vulture, Italy
[c] Department of Health Science, Human Pathology Section, University of Palermo School of Medicine, Palermo, Italy
[d] Department of Predictive and Preventive Medicine, Fondazione IRCCS Istituto Nazionale Dei Tumori, Milan, Italy
[e] Department of Oncology and Hemato-oncology, University of Milan, Milan, Italy
[f] Hematology Unit, Fondazione IRCCS Ca' Granda, Ospedale Maggiore Policlinico, Milan, Italy

ARTICLE INFO

Article history:
Received 11 July 2017
Received in revised form
15 September 2017
Accepted 16 September 2017

Keywords:
Thyroid carcinoma
COPZ1
Non-oncogene addiction
Cell death

ABSTRACT

Thyroid carcinoma is generally associated with good prognosis, but no effective treatments are currently available for aggressive forms not cured by standard therapy. To find novel therapeutic targets for this tumor type, we had previously performed a siRNA-based functional screening to identify genes essential for sustaining the oncogenic phenotype of thyroid tumor cells, but not required to the same extent for the viability of normal cells (non-oncogene addiction paradigm). Among those, we found the coatomer protein complex ζ1 (COPZ1) gene, which is involved in intracellular traffic, autophagy and lipid homeostasis. In this paper, we investigated the mechanisms through which COPZ1 depletion leads to thyroid tumor cell death. We showed that siRNA-mediated COPZ1 depletion causes abortive autophagy, endoplasmic reticulum stress, unfolded protein response and apoptosis. Interestingly, we observed that mouse tumor xenografts, locally treated with siRNA targeting COPZ1, showed a significant reduction of tumor growth. On the whole, we demonstrated for the first time the crucial role of COPZ1 in the viability of thyroid tumor cells, suggesting that it may be considered an attractive target for novel therapeutic approaches for thyroid cancer.

Introduction

Cancer cells often depend on non mutated genes and pathways to support their unchecked growth. The activity of these genes is essential for tumor cells, but not required to the same extent by normal cells; this concept is known as “non-oncogene addiction” (NOA) paradigm [1]. NOA genes represent tumor vulnerabilities and their inhibition results in the failure of the oncogenic phenotype. Nowadays, large-scale siRNA-based functional screening of cancer cell lines represent a powerful strategy for the identification of NOA genes that can be investigated as therapeutic targets for many types of tumors [2]. We used this approach to unveil nodal points for therapeutic intervention for thyroid carcinoma (TC), which represents the most frequent endocrine cancer, with a rapidly increasing incidence [3].

The majority of TC originates from epithelial cells and includes well-differentiated papillary (PTC) and follicular (FTC) carcinomas, poorly differentiated (PDTC) and undifferentiated anaplastic carcinomas (ATC). Most TCs are effectively treated by standard therapy, involving surgery, thyroid stimulating hormone and radioiodine. Nevertheless, a fraction of patients cannot be cured due to local recurrence (in up to 20% of patients), distant metastasis (in approximately 10% at 10 years [4]) and/or radioresistant disease.

☆ Supported by: Associazione Italiana per la Ricerca sul Cancro (AIRC) [Grant IG 11347, 2012; IG 18395, 2017] to A.Greco and by a Fondazione Umberto Veronesi Fellowship to M.C. Anania.

* Corresponding author. Fondazione IRCCS Istituto Nazionale dei Tumori, Via G.A. Amadeo, 42, 20133 Milan, Italy.
E-mail address: angela.greco@istitutotumori.mi.it (A. Greco).

https://doi.org/10.1016/j.canlet.2017.09.024
0304-3835/

Furthermore, patients with PDTC and ATC have a very poor prognosis, with survival of few months in the case of ATC [5,6]. Even though recent molecular findings allowed the development of several therapies designed to specifically target thyroid oncoproteins or their downstream pathways, this strategy showed modest results and only partial response [7,8]. Few or no therapeutic options are currently available for patients with aggressive and iodine-refractory thyroid tumors. Thus, there is a need to better understand the mechanisms of thyroid carcinogenesis and to improve the treatment of the most aggressive tumor forms not curable by standard therapy.

We have recently discovered several thyroid tumor cell vulnerabilities. By screening a siRNA library, we identified a set of genes whose silencing inhibited the growth of a panel of thyroid tumor cells, but not of normal immortalized thyrocytes. The COPZ1 gene was found among the top ranked genes [9]. COPZ1 (coatomer protein complex ζ1) belongs to the coatomer protein complex I (COPI), an heptameric complex which is involved in: assembly of coated vesicles on Golgi membranes, retrograde transport of luminal and membrane proteins in the ER-Golgi secretory pathway, endosome maturation, autophagy [10,11] and lipid homeostasis [12]. It has been demonstrated that COPZ1 knockdown causes cell death in both proliferating and nondividing tumor cells. Unlike tumor cells, normal cells are not sensitive to COPZ1 inhibition [13]. We identified COPZ1 as a thyroid tumor cell specific survival gene, as its inhibition induced cell death in tumor cell lines but not in immortalized thyrocytes. This evidence, together with a not significant variation of expression and absence of mutations in PTC, allowed us to classify COPZ1 as an example of "non-oncogene addiction" for thyroid cancer cells [9].

Here we investigated the mechanisms through which COPZ1 depletion leads to thyroid tumor cell death and explored its potential use as therapeutic target for thyroid carcinoma. We found that cell death induced by COPZ1 depletion is associated with abortive autophagy, ER stress, UPR and apoptosis. Interestingly, local treatment with siCOPZ1 oligos reduced tumor growth in an *in vivo* model of thyroid carcinogenesis.

Materials and methods

Cell lines

Thyroid tumor cell lines, primary thyrocytes and mammary epithelial h-TERT-HME1 cells were cultured as previously described [9,14,15]. Source and culture conditions are reported in Supplementary. GFP-LC3 stable cell lines were generated by transfecting 2 μg of pEGFP-LC3 plasmid (from Tamotsu Yoshimori's laboratory [16], using the Lipofectamine 3000 reagent (Invitrogen Life Technologies, Carlsbad, CA, USA) for TPC-1, and Lipofectamine LTX (Invitrogen Life Technologies) for 8505C cells, according to manufacturer's instruction. Transfected cells were selected and propagated in medium containing G418 (500 μg/ml, Invitrogen Life Technologies).

Detection of LC3 puncta

Cells growing on glass coverslips were transfected as described below and 24 h, 48 h, 72 h later fixed for 20 min with 4% paraformaldehyde. After washing with PBS, cells were treated with the ProLong Diamond Antifade mountant with DAPI (P36966, Molecular Probes, Invitrogen Life Technologies) and imaged with immunofluorescence microscopy (Eclipse E1000; Nikon Instruments, Inc. NY, USA). The percentage was calculated as the ratio between cells displaying LC3 puncta and total cells (at least 150), considering six randomly selected 60× fields.

siRNA reagents and transfection

siRNA transfection was performed using 20 nM of siRNA oligos (see list in Supplementary) and the Lipofectamine RNAiMAX reagent (Invitrogen Life Technologies), according to manufacturer's instruction.

Colony formation assay

Cells were plated in 100 mm dishes and transfected the following day with 20 nM of siRNAs. One day later, cells were collected and plated as follows: 2×10^4 cells in 24 well-plates for colony formation assay; 1.5×10^5 cells in 60 mm dishes for western blot analysis. For the colony formation assay, cells were fixed five days later with formaldehyde 3.7% v/v solution for 30 min, washed with PBS and stained for 20 min with 0.1% crystal violet (w/v). Pictures were taken using an Epson image scanner.

Western blot analysis

WB analysis was performed as previously described [17]. The list of antibodies is provided in Supplementary.

RNA extraction and real time PCR

RNA extraction and Real time PCR were performed as previously described [17]. The following TaqMan gene expression assays (Applied Biosystem, Foster City, CA) were used: Hs01023197_m1 for COPZ1 and Hs00358796_g1 for CHOP expression; Hs02800695_m1 for HPRT1, used as housekeeping gene for normalization among samples.

Apoptosis assay

Cells were transfected with 20 nM of siRNA oligos in the presence of 2 μM of the fluorogenic substrate for activated caspase-3/7 (CellEvent™ Caspase-3/7 Green Detection Reagent, Invitrogen Life Technologies). Live-cell fluorescence images were taken 72 h later with microscope (Eclipse TE2000-S; Nikon Instruments).

In vivo studies

Female CD-1 nu/nu mice (5-weeks old) (Charles River, Calco, Italy) were injected subcutaneously into the left flank with 8505C cells (10×10^6). When xenograft tumors reached the mean volume of 0.085 mm^3 (range 0.040–0.144), they were randomly divided into three groups and then locally treated with 20 μg of siCOPZ1 oligos (4457308, Ambion® ID s22427) or non-targeting oligos (4457289, Ambion® *In Vivo* Negative Control #1 siRNA) mixed in 50 μl of MaxSuppressor™ In Vivo RNA-LANCEr II reagent (Bioo Scientific, Austin, TX, USA), or with MaxSuppressor™ only. Treatments were carried out at day 17, 20, 23, 27, 30 after cell injections. Tumor growth was followed for 34 days and assessed by monitoring tumor weight (TW), as previously described [18]. Animal studies were reviewed and approved by the Ethics Committee for Animal Experimentation of the hosting institution and are in accordance with the guidelines of the UK Coordinating Committee for Cancer Research [19].

Immunohistochemistry

Serial sections from paraffin-embedded tumor xenografts (2-μm thick) were stained with hematoxylin and eosin and evaluated under a light microscope to assess the pattern of tumor growth. Antigen retrieval was performed using 1 mM citrate buffer (pH 6), then sections were immunostained with a primary rat polyclonal antibody anti-human COPZ1 (1:400 SAB4500896 Sigma-Aldrich St Louis, Mo, USA), anti-human Ki-67 (Mib1) (1:200 M7240 Dako, Agilent Technologies, CA, USA). Immunostains were performed using standard immunoperoxidase protocol followed by diaminobenzidine chromogen reaction (Dako REAL™ EnVision™ Detection System, K5007 Dako). The intensity of staining for COPZ1 was scored as low (1+), medium (2+) or high (3+). The percentage of cells immunostained for Ki67 and necrotic cells was estimated counting one 10× field, randomly selected. One sample of each group of tumor explants was excluded from the IHC analysis due to technical problems.

Gene/miRNA expression analysis

Gene expression data of *COPZ2* gene (log scale) from 58 normal-thyroid tissue samples compared to 31 ATC, 72 PTC and 17 PDTC samples, were obtained combining GSE3467 [20], GSE6004 [21], GSE33630 [22,23] and GSE76039 [24] publicly available datasets. Raw intensity expression values on U133 Plus 2.0 array (Affymetrix, Santa Clara, CA) were processed by Robust Multi-array Average procedure [25], with the re-annotated Chip Definition Files from BrainArray libraries version 20.0.0 [26], available at http://brainarray.mbni.med.umich.edu. Batch effects were removed by using sva R/Bioconductor package [27]. The analysis of the thyroid TCGA dataset from 58 paired normal/PTC samples was performed as previously described [9]. Normalized reads per million miRNA mapped (RPM) data were obtained for the same 58 tumor samples from Illumina HiSeq Level 3 isoform quantification files (TCGA Data Portal website), by summing up the reads aligned to each 3p or 5p miRBase v16 mature strands [28,29]. Pearson's correlation method was applied to evaluate the correlation between RNAseq normalized gene and miRNA read counts (log scale) in 58 tumor samples.

Results

COPZ1 depletion affects thyroid tumor cell viability

The issue that COPZ1 represents vulnerability for thyroid tumor cell lines but not for normal thyrocytes [9] is further documented

by the colony forming assay in Fig. 1A. Upon transfection of siRNA oligos targeting COPZ1 (siCOPZ1), a drastic growth inhibition was observed in thyroid tumor cell lines (PTC-derived: BCPAP and TPC-1; FTC-derived: WRO82-1; ATC-derived: 8505C, KAT-18, and HTC/C3) in comparison to non-targeting (siNT) transfected cells, and to COPZ1-depleted Nthy-ori 3-1 cells, normal immortalized thyrocytes. Western blot (WB) analysis performed in parallel documented the efficient COPZ1 silencing in all the cell lines (bottom panel). SiRNA transfected TPC-1, 8505C, HTC/C3, and Nthy-ori 3-1 cell lines were also analyzed by time-lapse phase-contrast video microscopy (Supplementary Videos). Unlike siNT-transfected cells, COPZ1-depleted tumor cells showed morphological changes, such as shrinking and rounding up 30 h (for TPC-1 cells) and 48 h (for 8505C and HTC/C3 cells) after silencing Then, cells detached from dishes and reached massive cell death at the end of the experiment (68 h for TPC-1 cells, 89 h for 8505C and HTC/C3 cells). None of

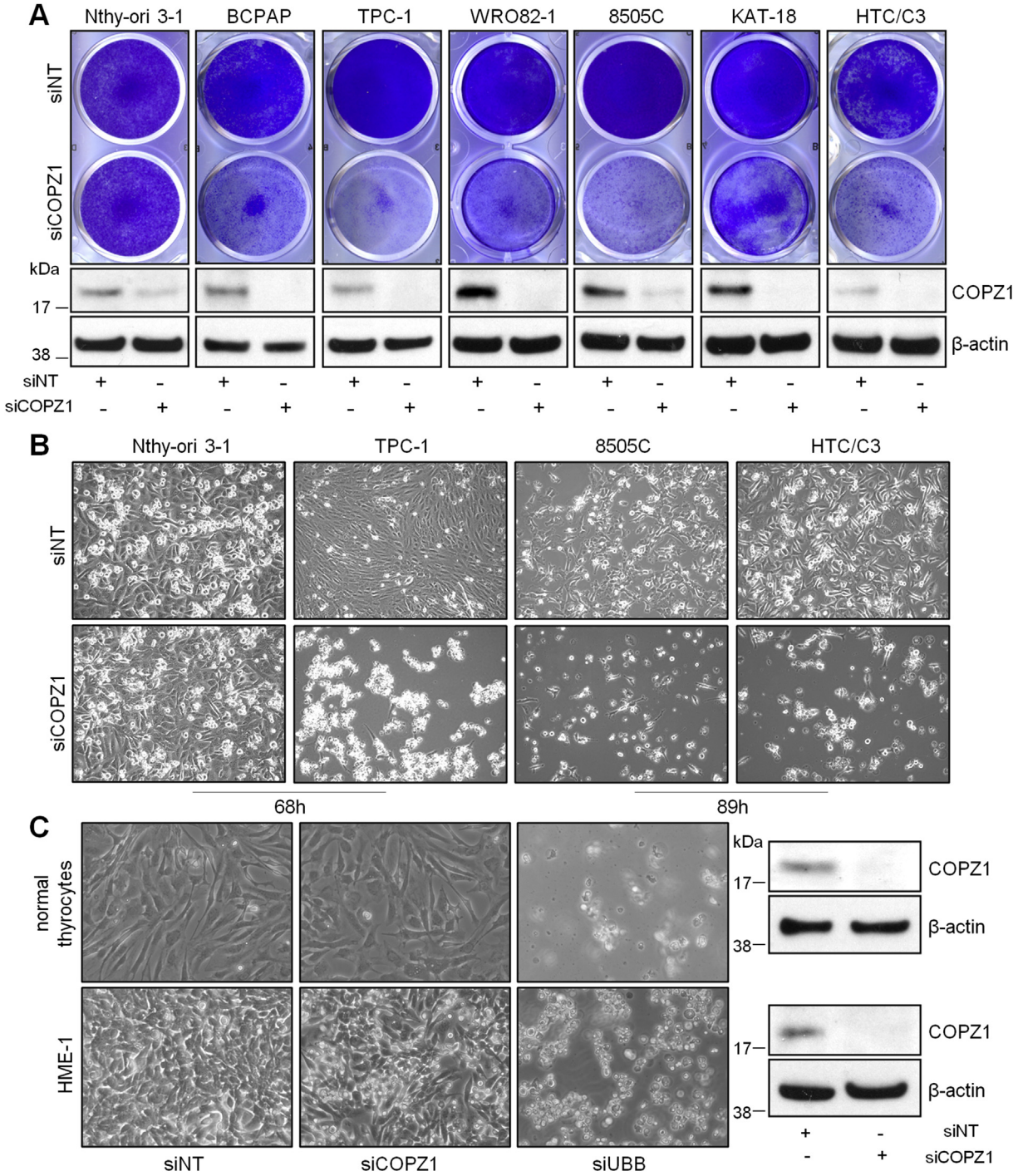

Fig. 1. Effect of COPZ1 silencing on cell viability. (A) Colony forming assay of thyroid cell lines, 5 days after siRNA transfection; (B-C) Representative pictures at 10× magnification of Nthy-ori 3-1, TPC-1, 8505C, HTC/C3 cells, primary normal thyrocytes and human mammary epithelial cells (HME-1) at the indicated time points after siRNA transfection. In (A) and (C), cells were assessed by WB for protein levels of COPZ1 72 h after siRNA transfection; β-actin was used for normalization of gel loading. siNT: Non-Targeting siRNAs; siCOPZ1: siRNAs targeting COPZ1; siUBB: siRNA targeting Ubiquitin B.

these effects was observed in COPZ1-depleted NThy-ori 3-1 cells, which proliferated as the control (siNT) and reached confluence at the end of the experiment (68 h). In Fig. 1B, representative images of each cell lines at the end of experiment are reported. Further images documenting cell morphological changes after COPZ1 depletion are shown in Supplementary Fig. S1. We also showed the lack of effect of COPZ1 silencing on primary human thyrocytes and human mammary epithelial HME-1 (Fig. 1C): COPZ1 depletion leaves unaffected the growth of these non malignant cells, similarly to the negative control siNT; on the contrary, a massive cell death was observed in cells transfected with siRNA oligos targeting Ubiquitin B (siUBB), used as control. WB analysis 72 h after siRNA transfection documented the complete abrogation of COPZ1 protein expression.

Supplementary data related to this article can be found online at https://doi.org/10.1016/j.canlet.2017.09.024

COPZ1 depletion affects autophagy

COPI complex members are involved in autophagy [11] and are required for completion of the autophagic process. Moreover, the depletion of COPI members impairs productive autophagy, as demonstrated in prostate, breast and ovarian carcinoma cells [13,30]. TPC-1 and 8505C cell lines, stably expressing the autophagosome marker GFP-LC3 (hereafter referred as TPC1-GL3 and 8505-GL3) were transfected with siCOPZ1 and siNT oligos and analyzed at different time points by fluorescence microscopy for the presence of the typical autophagy-associated LC3 puncta (Fig. 2A). The number of siNT-transfected cells displaying LC3 puncta remained low over the time. On the contrary, the number of COPZ1-depleted cells presenting puncta significantly increased over the time. In TPC1-GL3 cells puncta were detected in 5.7% and 38% at 24 h and 48 h, respectively; the analysis at 72 h was not feasible, as cells detached from glass coverslip due to the lethal effect of COPZ1 silencing. In 8505-GL3 cells, puncta were present in 6%, 14% and 34%, at 24 h, 48 h and 72 h, respectively. In Fig. 2B, representative images of COPZ1-depleted cells displaying LC3 puncta and relative controls are shown. Autophagosome formation upon COPZ1 silencing was also demonstrated by assessing the conversion of the endogenous LC3-I to LC3-II by WB. Accumulation of LC3-II protein was observed in COPZ1-depleted naive TPC-1 and 8505C cells. In both cell lines, the endogenous LC3-II was barely detectable at 48 h and progressively increased at the latest time points (Fig. 2C). Since an increased steady-state expression of LC3-II could suggest persistent accumulation of autophagosomes, impaired recycling and consequently block of the autophagic flux, we investigated whether COPZ1 depletion causes abortive autophagy. We monitored by WB whether LC3-II accumulation was associated with increased expression of SQSTM1/p62, an LC3-binding protein mainly degraded through autophagy catabolism and whose increase is a marker of abortive autophagy [31]. We observed an increase of SQSTM1/p62 in both COPZ1-depleted cell lines in comparison to controls (Fig. 2D). Such increase was 1.4 and 1.6 fold in TPC-1 cells at 72 h and 96 h, and 2.9 and 2.5 fold in 8505C cells. The persistent accumulation, rather than turnover/degradation of autophagosomes, and the concomitant increase of SQSTM1/p62 protein expression suggest that COPZ1 depletion is associated with abortive autophagy.

COPZ1 depletion induces endoplasmic reticulum stress and unfolded protein response

As COPZ1 regulates vesicular transport, its depletion could be associated with protein accumulation in the endoplasmic reticulum (ER) and with a deficit in proteins coming back from the Golgi. Since these effects could be linked to the activation of ER stress and of unfolded protein response (UPR), we investigated the expression of some components of these pathways. COPZ1-depleted TPC-1 and 8505C cells showed an increased expression of the chaperone GRP78/BiP, which, upon ER stress, is the major responsible for the activation of downstream UPR signals [32,33]. In TPC-1 cells, the level of GRP78/BiP increases by 1.5, 2.8 and 11 fold at 48 h, 72 h and 96 h after siRNA transfection, respectively, in comparison to the control; whereas, in 8505C cells the increase was by 1.8, 3.9 and 3.2 fold (Fig. 3A). Concomitantly, we observed an increase of another marker of ER stress, the ER lumen chaperone calnexin (1.2 at 48 h and 1.6 from 72 h fold increase in TPC-1; 1.4 and 2.8 fold increase in 8505C cells) (Fig. 3A). CHOP, also known as GADD153, is transcriptionally upregulated during ER stress and UPR [34,35]. We analyzed the expression of CHOP and COPZ1 by Real Time PCR in TPC-1 and 8505C cells at different time points after COPZ1 silencing. As shown in Fig. 3B, COPZ1 depletion led to a drastic increase of CHOP expression in comparison to the control. In conclusion, our data indicate that COPZ1 depletion causes the onset of ER stress and UPR.

COPZ1 depletion induces apoptotic cell death

Prolonged ER stress or failure of adaptive response can result in cell death [36]. Moreover, CHOP activation triggers apoptotic death [34,35]. TPC-1 and 8505C cells were transfected with siCOPZ1 or siNT oligos in the presence of the fluorescent substrate for activated caspase-3/7. Live-cell fluorescence microscopy performed 72 h after transfection showed a significant increase of Caspase-3/7 activity in COPZ1-depleted cells in comparison to the siNT control (Fig. 4A). The induction of apoptosis by siCOPZ1 is also documented by the WB analysis in Fig. 4B: COPZ1 depletion increases cleaved PARP and cleaved caspase-3 levels, which were detectable at 48 h and 72 h after siRNA transfection in TPC-1 and 8505C cells, respectively. Overall, these results suggest that the depletion of COPZ1 induces caspase-dependent apoptosis in thyroid tumor cells.

In vivo effects of COPZ1 depletion

We used 8505C cell mouse xenografts as *in vivo* model of thyroid carcinogenesis and, in a preliminary experiment, we tested the *in vivo* efficacy of siRNA targeting COPZ1. Nude mice were xenografted with 8505C cells and then locally treated with siCOPZ1, explanted and analyzed by WB three days later. As shown in Fig. 5A, a consistent reduction (by 40%) of COPZ1 protein in siCOPZ1-treated tumor in comparison to vehicle- or siNT-treated control was observed. The expression of COPZ1 protein in tumor explants was also analyzed by immunohistochemistry (IHC). The intensity of staining for COPZ1 in siCOPZ1 explant was reduced in comparison to siNT explant: score 1+ vs 3+. This was associated with a reduction of the rate of proliferating cells, determined by Ki67 staining: 15% in siCOPZ1 explant vs 50% in siNT explant (Fig. 5B). After proving the efficacy of siCOPZ1 in an *in vivo* setting, we evaluated the effect of COPZ1 silencing on *in vivo* tumor growth. Nude mice were xenografted with 8505C cells and, at day 17 after, they were locally treated twice a week with siCOPZ1, or with siNT, or with the vehicle only. At day 34, tumors were excised and weighted. As shown in Fig. 5C, treatment with siCOPZ1 significantly reduced tumor growth compared to siNT or vehicle treatments (controls). Then, tumor explants were analyzed by IHC for the expression of COPZ1 protein. COPZ1 immunostaining was high in two siNT samples and ranged from medium to high in two other samples. Conversely, in COPZ1-depleted explants it was very low (two samples), low with medium areas (two samples) or medium

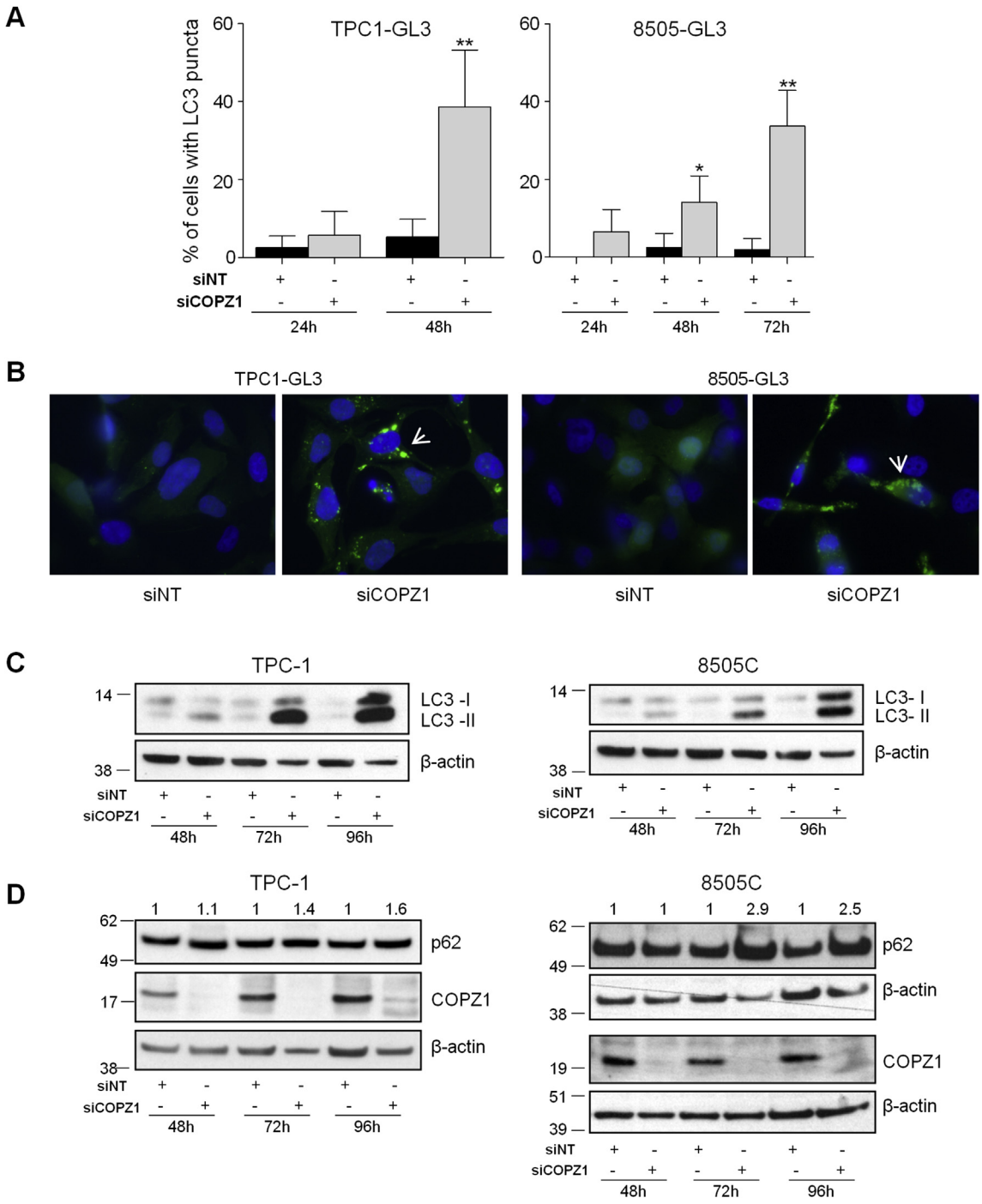

Fig. 2. Effect of COPZ1 silencing on autophagy. (A) Percentage of TPC1- and 8505C-GL3 cells displaying LC3 puncta at different time points after siCOPZ1 and siNT oligos transfection; the asterisks indicate differences significant by the unpaired Student's t-test (*P < 0.05, **P < 0.01). (B) Representative pictures of TPC1- 8505C-GL3 cells, 48 h and 72 h after siRNA transfection, respectively; cells were analyzed by fluorescence microscopy for the presence of LC3 puncta (green; arrows); nuclear DNA was stained with DAPI. (C-D) TPC-1 and 8505C cells were analyzed by WB for the expression of LC3-I/II, SQSTM1/p62 and COPZ1 proteins, at the indicated time points after siRNA transfection; β-actin was used for normalization of gel loading. In 8505C cells (D), p62 and COPZ1 expression in the same cell extracts was assessed in two separate gels.

(one sample). In line with this, the mean rate of proliferating cells (Ki67) was 53.7% for siNT and 31% for siCOPZ1 explants. Concomitantly, when we evaluated the neoplastic cellularity, we observed an increase of necrosis (20%) in siCOPZ1 explants in comparison with the controls (11.2%) (Fig. 5D). Representative pictures of selected explants are shown in Fig. 5E: the siNT-9 sample showed high COPZ1 and Ki67 (50%) expression and low necrotic cells (5%), whereas the siCOPZ1-19 sample displayed an opposite state, being the COPZ1 staining low, Ki67 20% and necrotic cells 25%. Overall, our results demonstrated that the local treatment with siCOPZ1 productively reduced tumor growth in our model of thyroid carcinoma in nude mice.

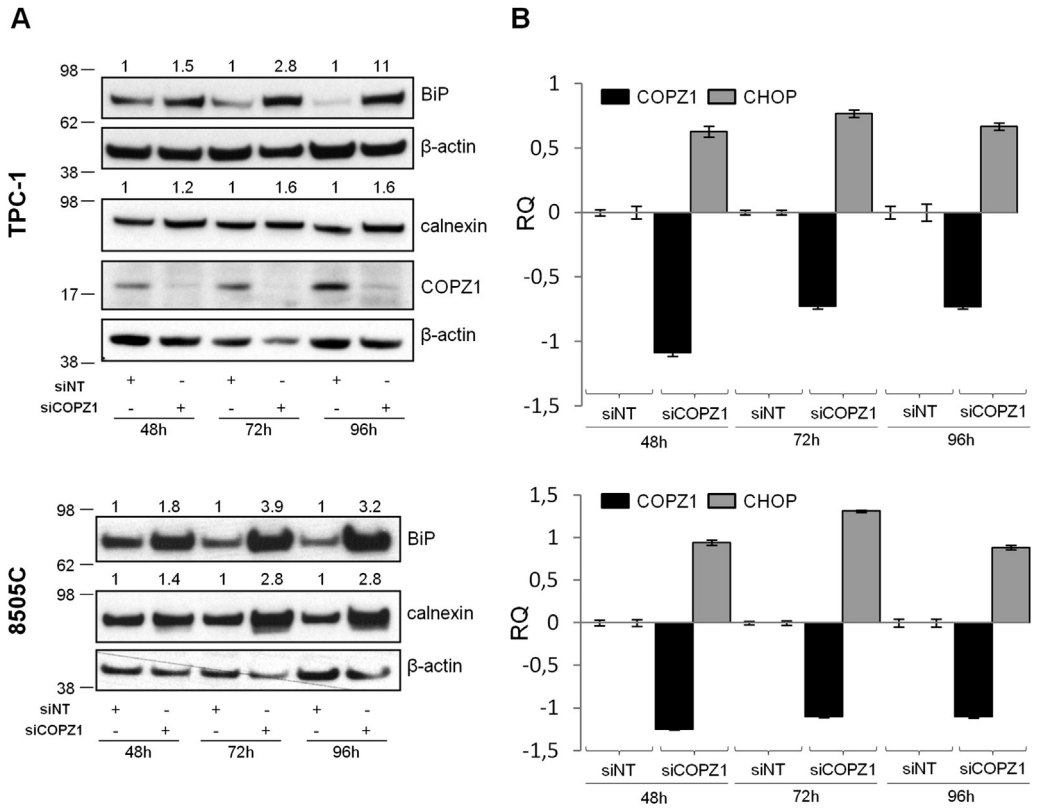

Fig. 3. Effect of COPZ1 silencing on ER stress and UPR. (A) WB analysis of calnexin and BiP protein expression in TPC-1 and 8505C cells, at the indicated time points after siRNA transfection; β-actin was used for normalization of gel loading. In TPC-1 cells, calnexin, COPZ1 and BiP expression in the same cell extracts was assessed in two separate gels; in 8505C cells, calnexin and BiP expression was assessed in the same gel of Fig. 2D. (B) Real-time PCR analysis of COPZ1 and CHOP gene expression in TPC-1 and 8505C cells at the indicated time points after siRNA transfection; results are presented as log10-transformed relative quantity (RQ) of COPZ1/CHOP mRNA normalized for HPRT1 housekeeping gene expression. Data represent the mean ± sd of two independent experiments.

COPZ2 is downregulated in thyroid cancers

COPZ1 vulnerability is related to downregulation of the paralogous *COPZ2* gene in tumor cells. While normal cells tolerate COPZ1 inhibition because COPZ2 can replaces its activity in the COPI complex, the absence of COPZ2 in tumor cells confers sensitivity to COPZ1 depletion. Interestingly, *COPZ2* was found downregulated in several primary tumors compared to their normal counterparts [13]. We have previously provided evidence that dependence of thyroid tumor cell lines on COPZ1 may result from downregulation of *COPZ2*, since *COPZ2* mRNA expression is downregulated in the majority of analyzed thyroid tumor cell lines [9]. In order to assess whether also thyroid tumors belonging to different histotypes may be sensitive to COPZ1 targeting, we interrogated several publicly available datasets for the expression status of *COPZ2*. The first analysis combined data from different datasets, including 58 normal thyroid, 72 PTC, 17 PDTC and 31 ATC samples [20–24]: *COPZ2* was found downregulated in all the tumor histotypes (Fig. 6A). Furthermore, COPZ2 gene was significantly downregulated in the 58 PTC samples from the thyroid TCGA dataset [28], compared to the paired normal counterpart (Fig. 6B, left). Therefore, the frequent downregulation of COPZ2 in thyroid tumors allow predicting their sensitivity to COPZ1 inhibition.

The first intron of the *COPZ2* gene encodes the precursor of miR-152 [37], which exerts a tumor suppressor role and is frequently downregulated in several tumors. miR-152 and its hosting gene *COPZ2* are transcribed from the same promoter and are concurrently silenced in tumor cells [13]. To assess mirR-152 expression in thyroid tumors, data were retrieved from TCGA and correlated with *COPZ2* expression. The analysis shows a notable positive correlation between *COPZ2* and hsa-miR-152 RNAseq expression levels (Fig. 6B, right). This result indicates that miR-152, concurrently to *COPZ2*, is downregulated in thyroid cancer and it may exert an oncosuppressor role also in this tumor type.

Discussion

By performing a siRNA-based functional screening, we have recently discovered several thyroid tumor cell vulnerabilities, consisting in a set of genes, defined non-oncogenes, whose silencing inhibited the growth of a panel of thyroid tumor cells, but not that of normal immortalized thyrocytes. The COPZ1 gene was found among the top significant genes, exerting a role in sustaining the phenotype of thyroid tumor cells. In this study, we dissected the mechanisms leading to cell lethality upon COPZ1 depletion and explored its employability as therapeutic target for thyroid carcinoma.

First, we confirmed that COPZ1 represents vulnerability for several thyroid tumor cell lines since its silencing drastically impairs their viability and demonstrated the lack of effect also in normal primary thyrocytes and mammary epithelial cells.

Our study, aimed at better characterizing the mechanisms leading to cell death upon COPZ1 depletion, showed that, similarly to other members of the coatomer complex [11,30], COPZ1 was a critical player of autophagy. Indeed, COPZ1 silencing initiated autophagy, which became abortive due to an increase rather than a turnover of autophagosomes. Concomitantly, COPZ1-depleted cells displayed the activation of markers of ER stress and UPR. Whether

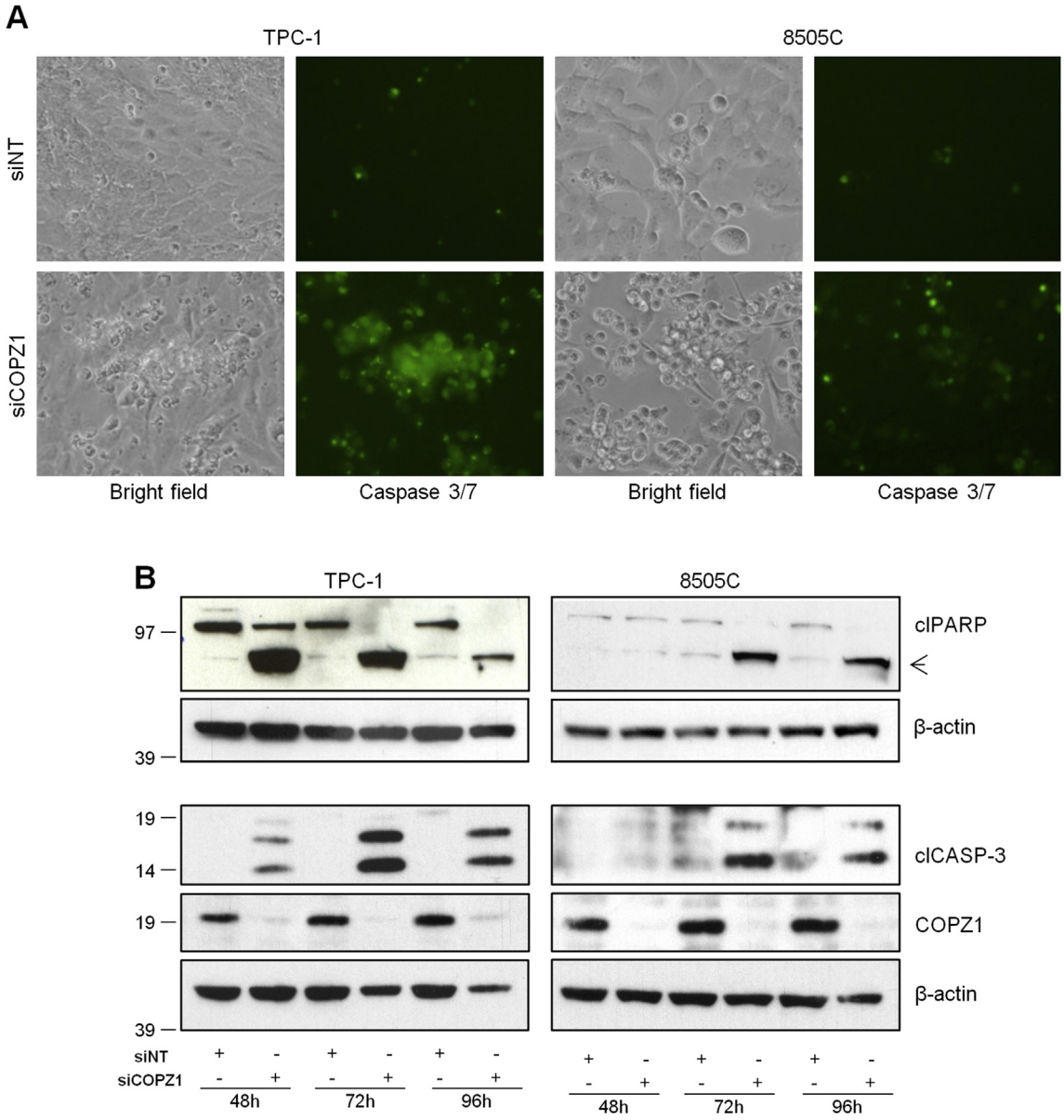

Fig. 4. Effect of COPZ1 silencing on cell death. (A) TPC-1 and 8505C cells were transfected with siCOPZ1 or siNT oligos in the presence of 2 μM of the fluorogenic substrate for activated caspase-3/7; live-cell fluorescence images (10× magnification) were taken 72 h later with microscope. (B) WB analysis of cleaved PARP (arrowhead), cleaved caspase 3 and COPZ1 protein expression, at the indicated time points after siRNA transfection; β-actin was used for normalization of gel loading. Cleaved PARP expression in the same cell extracts was assessed in two separate gels.

the impairment of autophagy is the cause or the consequence of ER stress remains to be investigated. We then demonstrated that the onset of a prolonged ER stress exacerbates cell death, since COPZ1-depleted cells rapidly underwent caspase-dependent apoptosis.

Interestingly, in support to what observed by functional studies, a preliminary gene expression profiling of COPZ1-depleted 8505C cells indicated that the main upregulated canonical pathways consist of the unfolded protein and ER stress response, lipid metabolism and cell death (apoptosis). In parallel, proteomic profiling of COPZ1-depleted 8505C cells by nano-scale liquid chromatographic tandem mass spectrometry, indicated that the main involved pathways deal with vesicle trafficking, autophagy and caspase cascade in apoptosis (our unpublished results), in keeping with what observed by gene expression analysis.

Our results suggest that thyroid tumor cells dependence upon the activity of COPZ1 may be related to its pivotal involvement on the regulation of autophagy, UPR and ER stress, processes generally known as cytoprotective and adaptive mechanisms for cancer cell survival. Thus, COPZ1 inhibition may represent a strategy to target these processes and convert their effect into a lethal mechanism. Interestingly, normal cells, which are probably not strictly dependent on these mechanisms, are preserved from cell death. However, apart from the well known role of COPZ1 in vesicle trafficking, the possible direct involvement of COPZ1 in cancer cell survival is still unclear. How COPZ1 depletion modulates the activation of intracellular multiple signalling pathways, executors of the final lethal effect, remains to be better investigated. This will allow identifying other critical nodes in the oncogenic network whose inhibition will result in cell collapse.

In our study, the most striking effect of COPZ1 silencing was observed in mouse tumor 8505C xenografts: in fact, siCOPZ1-treated tumors showed a consistent reduction of tumor growth.

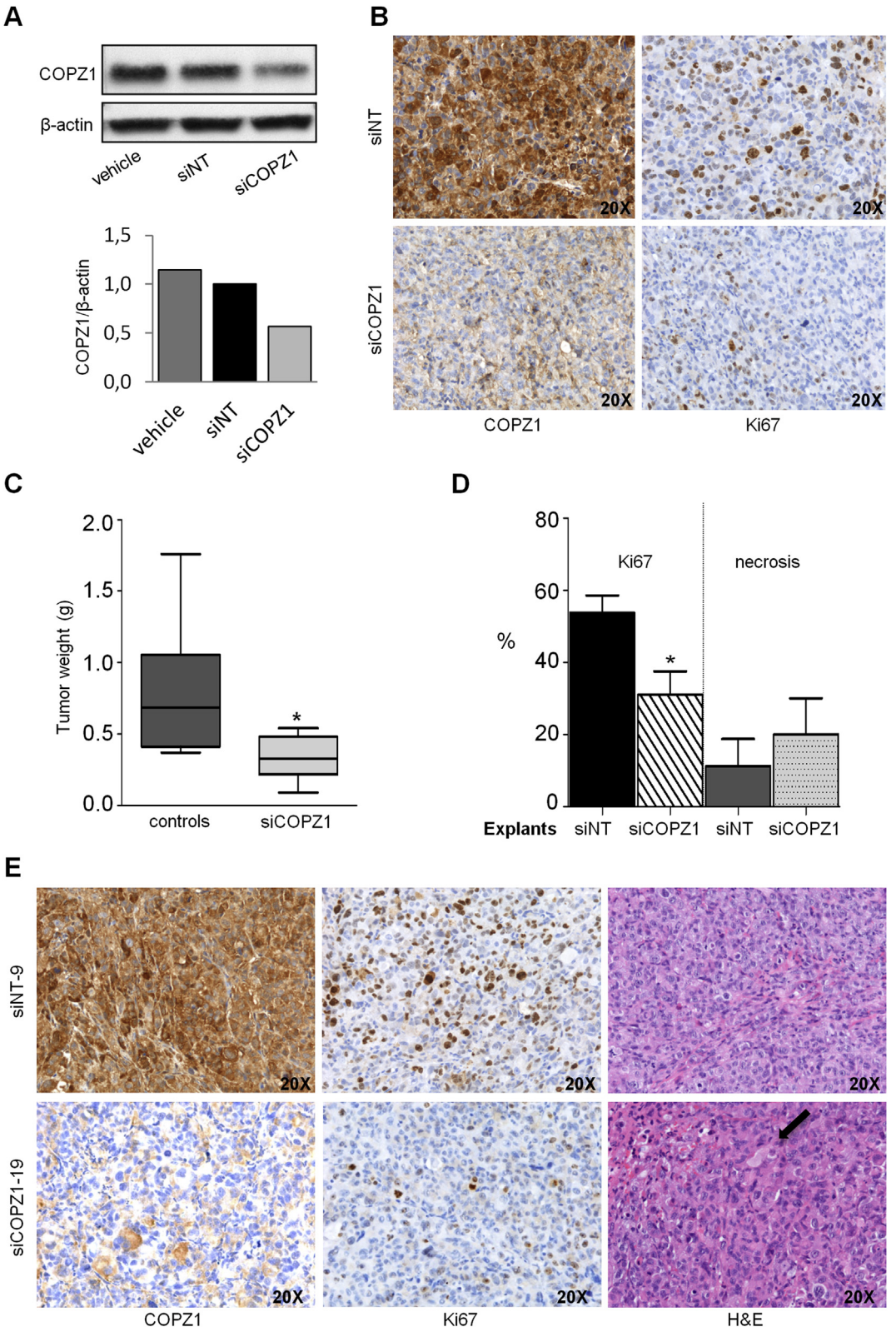

Fig. 5. Effect of COPZ1 silencing on 8505C *in vivo* tumor growth. (A) WB analysis of COPZ1 expression in tumor xenografts, excised three days after siRNA treatment; actin was used as loading control for cell extracts. The graph represents the densitometric analysis of the bands; data are reported as ratio of COPZ1 to actin and normalized for the siNT sample value. (B) IHC analysis of COPZ1 and Ki67 expression in siNT and siCOPZ1 tumor explants. (C) *In vivo* tumorigenicity assay: the line within each box represents the median tumor weight (g) value of 10 controls (five vehicle and five siNT) and six siCOPZ1 treated explants at the end of the experiment (34 days); upper and lower edges of each box represent the 75th and 25th percentile, respectively; upper and lower bars indicate the highest and lowest values less than one interquartile range from the extremes of the box. $^{*}P = 0.026$, controls vs. siCOPZ1-treated mice, Kruskal-Wallis Test. (D) Mean percentage of Ki67 positive and necrotic cells in tumor explants (four siNT and five siCOPZ1 samples); the asterisk indicates differences significant by the unpaired Student's t-test ($^{*}P < 0.05$). (E) IHC analysis of COPZ1 and Ki67 expression and H&E staining of two representative tumor explants (siNT-9, siCOPZ1-19); black arrow indicates areas of necrosis.

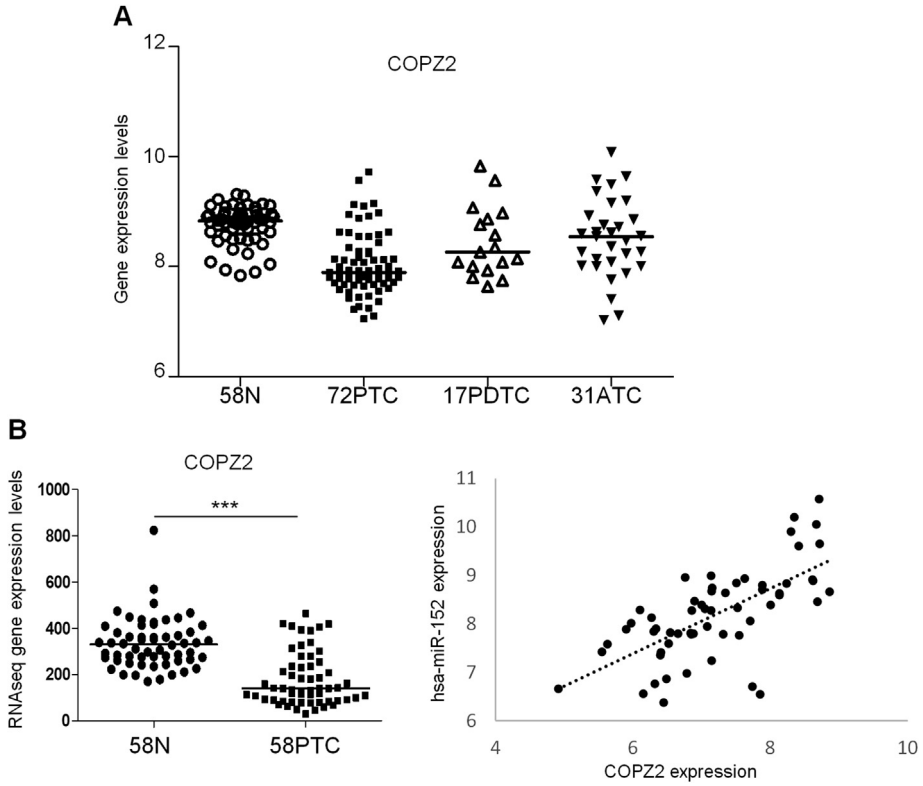

Fig. 6. Expression of *COPZ2* and mir-152 in thyroid carcinomas. (A) Scatter plot distribution of *COPZ2* gene expression levels (log_2 scale) in 58 normal thyroid-tissues, 72 PTC, 17 PDTC and 31 ATC primary tumor samples; in the graph the median is recorded. Nonparametric pairwise multiple comparisons between all analyzed groups were performed by Dunn's test and Benjamini-Hochberg correction, following a significant Kruskal-Wallis test ($p = 5.733\ e^{-11}$). (B) (left) Scatter plot distribution of RNAseq normalized expression values (natural scale) from the thyroid TCGA dataset of *COPZ2* in 58 matched normal (N) and PTC samples. Illumina HiSeq Level 3 data were downloaded from TCGA Data Portal website and RSEM gene normalized expression values were derived for 58 PTC patients, in tumor and adjacent normal samples, respectively; in the graph the median is recorded. Differential gene expression levels between tumor and normal groups were evaluated by Wilcoxon test (p-value $= 2.442 \times 10^{-10}$); (right) dispersion plot of *COPZ2* (x-axis) and hsa-miR-152 (y-axis) RNAseq normalized expression levels (log_2 scale) in the 58 PTC samples. Normalized reads per million miRNA mapped (RPM) data were obtained for the same 58 tumor samples from Illumina HiSeq Level 3 isoform quantification files (TCGA Data Portal website), by summing up the reads aligned to each 3p or 5p miRBase v16 mature strands. Pearson's correlation method was applied to evaluate the correlation between RNAseq normalized gene and miRNA read counts in 58 tumor samples ($r = 0.67$, p-value $= 8.41 \times 10^{-9}$).

Moreover, IHC analysis of tumor explants showed that COPZ1 silencing was associated with the decrease of the proliferative marker Ki67 and with an increase of necrosis. Further studies are needed to identify the mediators mainly involved in this process. An attractive hypothesis is that COPZ1 depletion could establish an inflammatory microenvironment through the release of cytokines/chemokines; this is supported by gene expression profile of COPZ1-depleted cells, showing upregulation of genes coding for cytokines involved in mediating communication between immune cells. More information on mediators released after cell death will be provided by the characterization of the cellular secretome content after COPZ1 depletion.

Tumor cell sensitivity to COPZ1 depletion is related to down-regulation of its paralogous COPZ2 gene. COPZ1 inhibition is tolerated by normal cells because COPZ2 substitutes for it in the COPI complex, whereas tumor cells, characterized by the absence of COPZ2, display sensitivity. This “synthetic lethality” renders COPZ1 depletion an attractive strategy to kill tumor cells. By interrogating publicly available data sets including a large collection of thyroid tumors we found that *COPZ2* was frequently downregulated in PTC, PDTC and ATC samples, thus indicating that the majority of thyroid tumors may be eligible for COPZ1 targeting. As reported in other tumor types [13], we observed a concomitant low expression of miR-152, encoded within the *COPZ2* gene, which exerts a tumor suppressor role and is donwnregulated in different tumors, including thyroid ones [38]. Whether the downregulation of *COPZ2* and miR-152 in thyroid tumors is due to promoter hypermethylation, as reported for other tumor types [39], remains to be investigated. Moreover, we cannot exclude that COPZ1 dependency of thyroid tumors may also rely on other mechanisms or on other components of the COPI complex. Indeed, we had previously observed that the FTC-derived WRO82-1 cell line is sensitive to COPZ1 depletion, even though it expresses high level of COPZ2 mRNA [9].

Recent reports indicate that, as for COPZ1, targeting other COPI complex members may represent a therapeutic approach for cancer. A siRNA-based functional screening proposed COPA gene, encoding the α subunit of COPI complex, as a potential therapeutic target for mesothelioma [40]. Claerhout et al. have shown that targeting the COPI complex members is a potent approach to block productive autophagy and stimulate cell death in cancer cells [30]. Recently, ARCN1, the δ-subunit of the COPI complex, has been proposed as a new therapeutic target [41]. COPB2 was found as synthetic lethal partner of mutated KRAS [42]. The co-occurrence of mutations in *KRAS* and *LKB1*, present in a small fraction of lung adenocarcinomas, drives addiction to the COPI complex members [43]. Of note, COPE gene, encoding the ε subunit of COPI complex, emerged from our screening in the list of genes specifically inhibiting thyroid tumor cell growth [9]. All this evidence suggests that targeting the coatomer complex, and consequently causing abortive autophagy and ER stress, may represent an optimal strategy to kill cancer cells, especially those resistant to conventional therapy.

In conclusion, we demonstrated that COPZ1 represents vulnerability for thyroid tumor cells, thus providing the first evidence of non-oncogene addiction for this tumor type. This adds a new element to the list of potential therapeutic targets, which includes, in addition to the driver oncogenic proteins and downstream pathways, several genes and miRNAs differentially expressed in thyroid tumors, some of which identified by our group [17,18,44–47], and whose role in promoting or suppressing the transformation process has been functionally demonstrated. On the whole, our results pave the way for designing novel therapeutic approaches based on COPZ1 inhibition useful for thyroid tumor patients who do not respond to standard therapies and rapidly progress to malignant forms. Notably, being effective on tumor but not on normal cells, these novel therapeutic approaches may have limited side effects.

Author contribution

AMC conceived the study, designed and performed the experiments, interpreted data and wrote the manuscript; CE, TK, GA, MG, DMT, CL and PS performed the experiments; LD performed the experiments and provided the editing of the manuscript; BB, TC, MG and NA supervisioned the study and revised the manuscript; GA conceived and supervisioned the study, wrote the manuscript.

Acknowledgements

We thank Prof. Nica Borgese and Dr.Sara Colombo (CNR Institute of Neuroscience, Milan, Italy), Dr. Italia Bongarzone (Fondazione IRCCS Istituto Nazionale dei Tumori, Milan, Italy) for their unconditional help. We also thank the Immunohistochemistry Facility of Fondazione IRCCS Istituto Nazionale dei Tumori, Milan, Italy. This work was supported by Associazione Italiana per la Ricerca sul Cancro (AIRC) [Grant IG 11347, 2012; IG 18395, 2017] to A.Greco and by a Fondazione Umberto Veronesi Fellowship to M.C. Anania.

Conflict of interest

None.

Appendix A. Supplementary data

Supplementary data related to this article can be found at https://doi.org/10.1016/j.canlet.2017.09.024.

References

[1] J. Luo, N.L. Solimini, S.J. Elledge, Principles of cancer therapy: oncogene and non-oncogene addiction, Cell 136 (2009) 823–837.
[2] R. Nagel, E.A. Semenova, A. Berns, Drugging the addict: non-oncogene addiction as a target for cancer therapy, EMBO Rep. 17 (2016) 1516–1531.
[3] G. Pellegriti, F. Frasca, C. Regalbuto, S. Squatrito, R. Vigneri, Worldwide increasing incidence of thyroid cancer: update on epidemiology and risk factors, J. Cancer Epidemiol. 2013 (2013), 965212.
[4] C.F. Eustatia-Rutten, E.P. Corssmit, N.R. Biermasz, A.M. Pereira, J.A. Romijn, J.W. Smit, Survival and death causes in differentiated thyroid carcinoma, J. Clin. Endocrinol. Metab. 91 (2006) 313–319.
[5] R.C. Smallridge, L.A. Marlow, J.A. Copland, Anaplastic thyroid cancer: molecular pathogenesis and emerging therapies, Endocr. Relat. Cancer 16 (2009) 17–44.
[6] M. Ragazzi, A. Ciarrocchi, V. Sancisi, G. Gandolfi, A. Bisagni, S. Piana, Update on anaplastic thyroid carcinoma: morphological, molecular, and genetic features of the most aggressive thyroid cancer, Int. J. Endocrinol. 2014 (2014), 790834.
[7] S.I. Sherman, Targeted therapies for thyroid tumors, Mod. Pathol. 24 (Suppl. 2) (2011) S44–S52.
[8] K.C. Bible, M. Ryder, Evolving Molecularly Targeted Therapies for Advanced-stage Thyroid Cancers, 2016.
[9] M.C. Anania, F. Gasparri, E. Cetti, I. Fraietta, K. Todoerti, C. Miranda, et al., Identification of thyroid tumor cell vulnerabilities through a siRNA-based functional screening, Oncotarget 6 (2015) 34629–34648.
[10] R. Beck, M. Rawet, F.T. Wieland, D. Cassel, The COPI system: molecular mechanisms and function, FEBS Lett. 583 (2009) 2701–2709.
[11] M. Razi, E.Y. Chan, S.A. Tooze, Early endosomes and endosomal coatomer are required for autophagy, J. Cell Biol. 185 (2009) 305–321.
[12] M. Beller, C. Sztalryd, N. Southall, M. Bell, H. Jackle, D.S. Auld, et al., COPI complex is a regulator of lipid homeostasis, PLoS Biol. 6 (2008), e292.
[13] M. Shtutman, M. Baig, E. Levina, G. Hurteau, C.U. Lim, E. Broude, et al., Tumor-specific silencing of COPZ2 gene encoding coatomer protein complex subunit zeta 2 renders tumor cells dependent on its paralogous gene COPZ1, Proc. Natl. Acad. Sci U.S.A. 108 (2011) 12449–12454.
[14] F. Curcio, F.S. Ambesi-Impiombato, G. Perrella, H.G. Coon, Long-term culture and functional characterization of follicular cells from adult normal human thyroids, Proc. Natl. Acad. Sci. U. S. A. 91 (1994) 9004–9008.
[15] A. Conti, M.T. Majorini, E. Fontanella, A. Bardelli, M. Giacca, D. Delia, et al., Lemur tyrosine kinase 2 (LMTK2) is a determinant of cell sensitivity to apoptosis by regulating the levels of the BCL2 family members, Cancer Lett. 389 (2017) 59–69.
[16] Y. Kabeya, N. Mizushima, T. Ueno, A. Yamamoto, T. Kirisako, T. Noda, et al., LC3, a mammalian homologue of yeast Apg8p, is localized in autophagosome membranes after processing, EMBO J. 19 (2000) 5720–5728.
[17] M.G. Vizioli, M. Sensi, C. Miranda, L. Cleris, F. Formelli, M.C. Anania, et al., IGFBP7: an oncosuppressor gene in thyroid carcinogenesis, Oncogene 29 (2010) 3835–3844.
[18] M.C. Anania, M. Sensi, E. Radaelli, C. Miranda, M.G. Vizioli, S. Pagliardini, et al., TIMP3 regulates migration, invasion and in vivo tumorigenicity of thyroid tumor cells, Oncogene 30 (2011) 3011–3023.
[19] U.K., Coordinating Committee on Cancer Research, UKCCCR guide lines for the welfare of animals in experimental neoplasia, Br. J. Cancer 58 (1988) 109–113.
[20] H. He, K. Jazdzewski, W. Li, S. Liyanarachchi, R. Nagy, S. Volinia, et al., The role of microRNA genes in papillary thyroid carcinoma, Proc. Natl. Acad. Sci. U.S.A. 102 (2005) 19075–19080.
[21] V. Vasko, A.V. Espinosa, W. Scouten, H. He, H. Auer, S. Liyanarachchi, et al., Gene expression and functional evidence of epithelial-to-mesenchymal transition in papillary thyroid carcinoma invasion, Proc. Natl. Acad. Sci. U.S.A. 104 (2007) 2803–2808.
[22] G. Dom, M. Tarabichi, K. Unger, G. Thomas, M. Oczko-Wojciechowska, T. Bogdanova, et al., A gene expression signature distinguishes normal tissues of sporadic and radiation-induced papillary thyroid carcinomas, Br. J. Cancer 107 (2012) 994–1000.
[23] G. Tomas, M. Tarabichi, D. Gacquer, A. Hebrant, G. Dom, J.E. Dumont, et al., A general method to derive robust organ-specific gene expression-based differentiation indices: application to thyroid cancer diagnostic, Oncogene 31 (2012) 4490–4498.
[24] I. Landa, T. Ibrahimpasic, L. Boucai, R. Sinha, J.A. Knauf, R.H. Shah, et al., Genomic and transcriptomic hallmarks of poorly differentiated and anaplastic thyroid cancers, J. Clin. Invest. 126 (2016) 1052–1066.
[25] R.A. Irizarry, B. Hobbs, F. Collin, Y.D. Beazer-Barclay, K.J. Antonellis, U. Scherf, et al., Exploration, normalization, and summaries of high density oligonucleotide array probe level data, Biostatistics 4 (2003) 249–264.
[26] M. Dai, P. Wang, A.D. Boyd, G. Kostov, B. Athey, E.G. Jones, et al., Evolving gene/transcript definitions significantly alter the interpretation of GeneChip data, Nucleic Acids Res. 33 (2005), e175.
[27] J.T. Leek, W.E. Johnson, H.S. Parker, A.E. Jaffe, J.D. Storey, The sva package for removing batch effects and other unwanted variation in high-throughput experiments, Bioinformatics 28 (2012) 882–883.
[28] The Cancer Gene Atlas Research Network, Integrated genomic characterization of papillary thyroid carcinoma, Cell 159 (2014) 676–690.
[29] C.F. Davis, C.J. Ricketts, M. Wang, L. Yang, A.D. Cherniack, H. Shen, et al., The somatic genomic landscape of chromophobe renal cell carcinoma, Cancer Cell 26 (3) (2014) 319–330.
[30] S. Claerhout, B. Dutta, W. Bossuyt, F. Zhang, C. Nguyen-Charles, J.B. Dennison, et al., Abortive autophagy induces endoplasmic reticulum stress and cell death in cancer cells, PLoS.One 7 (2012), e39400.
[31] G. Bjorkoy, T. Lamark, S. Pankiv, A. Overvatn, A. Brech, T. Johansen, Monitoring autophagic degradation of p62/SQSTM1, Methods Enzymol. 452 (2009) 181–197.
[32] J. Li, M. Ni, B. Lee, E. Barron, D.R. Hinton, A.S. Lee, The unfolded protein response regulator GRP78/BiP is required for endoplasmic reticulum integrity and stress-induced autophagy in mammalian cells, Cell Death Differ. 15 (2008) 1460–1471.
[33] J. Li, A.S. Lee, Stress induction of GRP78/BiP and its role in cancer, Curr. Mol. Med. 6 (2006) 45–54.
[34] E. Szegezdi, S.E. Logue, A.M. Gorman, A. Samali, Mediators of endoplasmic reticulum stress-induced apoptosis, EMBO Rep. 7 (2006) 880–885.
[35] N. Hiramatsu, W.C. Chiang, T.D. Kurt, C.J. Sigurdson, J.H. Lin, Multiple mechanisms of unfolded protein response-induced cell death, Am. J. Pathol. 185 (2015) 1800–1808.
[36] D.G. Breckenridge, M. Germain, J.P. Mathai, M. Nguyen, G.C. Shore, Regulation of apoptosis by endoplasmic reticulum pathways, Oncogene 22 (2003) 8608–8618.
[37] A. Rodriguez, S. Griffiths-Jones, J.L. Ashurst, A. Bradley, Identification of mammalian microRNA host genes and transcription units, Genome. Res. 14 (2004) 1902–1910.

[38] D. Cong, M. He, S. Chen, X. Liu, X. Liu, H. Sun, Expression profiles of pivotal microRNAs and targets in thyroid papillary carcinoma: an analysis of the cancer genome Atlas, Onco. Targets. Ther. 8 (2015) 2271–2277.
[39] T. Tsuruta, K. Kozaki, A. Uesugi, M. Furuta, A. Hirasawa, I. Imoto, et al., miR-152 is a tumor suppressor microRNA that is silenced by DNA hypermethylation in endometrial cancer, Cancer Res. 71 (2011) 6450–6462.
[40] H. Sudo, A.B. Tsuji, A. Sugyo, M. Kohda, C. Sogawa, C. Yoshida, et al., Knockdown of COPA, identified by loss-of-function screen, induces apoptosis and suppresses tumor growth in mesothelioma mouse model, Genomics 95 (2010) 210–216.
[41] D. Oliver, H. Ji, P. Liu, A. Gasparian, E. Gardiner, S. Lee, et al., Identification of novel cancer therapeutic targets using a designed and pooled shRNA library screen, Sci. Rep. 7 (2017), 43023.
[42] E.G. Christodoulou, H. Yang, F. Lademann, C. Pilarsky, A. Beyer, M. Schroeder, Detection of COPB2 as a KRAS synthetic lethal partner through integration of functional genomics screens, Oncotarget 8 (2017) 34283–34297.
[43] H.S. Kim, S. Mendiratta, J. Kim, C.V. Pecot, J.E. Larsen, I. Zubovych, et al., Systematic identification of molecular subtype-selective vulnerabilities in non-small-cell lung cancer, Cell 155 (2013) 552–566.
[44] M.C. Anania, C. Miranda, M.G. Vizioli, M. Mazzoni, L. Cleris, S. Pagliardini, et al., S100A11 overexpression contributes to the malignant phenotype of papillary thyroid carcinoma, J. Clin. Endocrinol. Metab. 98 (2013) E1591–E1600.
[45] C. Ferrario, P. Lavagni, M. Gariboldi, C. Miranda, M. Losa, L. Cleris, et al., Metallothionein 1G acts as an oncosupressor in papillary thyroid carcinoma, Lab. Invest. 88 (2008) 474–481.
[46] E. Minna, P. Romeo, L. De Cecco, M. Dugo, G. Cassinelli, S. Pilotti, et al., miR-199a-3p displays tumor suppressor functions in papillary thyroid carcinoma, Oncotarget 5 (2014) 2513–2528.
[47] E. Minna, P. Romeo, M. Dugo, L. De Cecco, K. Todoerti, S. Pilotti, et al., miR-451a is underexpressed and targets AKT/mTOR pathway in papillary thyroid carcinoma, Oncotarget 7 (2016) 12731–12747.